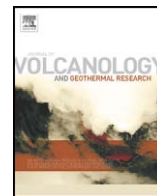




Contents lists available at ScienceDirect

## Journal of Volcanology and Geothermal Research

journal homepage: [www.elsevier.com/locate/jvolgeores](http://www.elsevier.com/locate/jvolgeores)Early Yellowstone hotspot magmatism and gold metallogeny<sup>☆</sup>Willis Hames<sup>a,\*</sup>, Derick Unger<sup>a,b</sup>, James Saunders<sup>a</sup>, George Kamenov<sup>c</sup><sup>a</sup> Department of Geology and Geography, Auburn University, Auburn, Alabama, USA<sup>b</sup> Newmont Mining Corp., Midas Operations, HC 66 Box 125, Midas, Nevada 89414, USA<sup>c</sup> Department of Geological Sciences, University of Florida, Gainesville, Florida, USA

## ARTICLE INFO

## Article history:

Received 19 May 2008

Accepted 20 July 2009

Available online xxxxx

## Keywords:

<sup>40</sup>Ar/<sup>39</sup>Ar geochronology

Lead isotopes

Adularia

Gold

## ABSTRACT

High-grade epithermal gold deposits in the Northern Great Basin have long been associated with regional Miocene basaltic to rhyolitic volcanism. Previous models for the low-sulfidation epithermal gold ores in this region have generally portrayed the bimodal magmas as a source of heat to drive large-scale convection of meteoritic water that leached gold from crustal sources and deposited it in hydrothermal vein systems, or required that the gold evolve from fractionated silicic magmas. New data of the present study indicate a more direct genetic link to the plume-related basaltic magmas of the region.

Laser <sup>40</sup>Ar/<sup>39</sup>Ar incremental heating plateau ages for single crystals of adularia from several of these low-sulfidation epithermal gold deposits range from 16.6 Ma to 15.5 Ma. Adularia from the Jumbo deposit yields three concordant plateau ages with a combined statistical result of 16.54 ± 0.04 Ma (95% confidence level, MSWD = 0.23). Plateau ages for adularia from other deposits in the region, and from gold-bearing veins in the Owyhee Mountains of southwestern Idaho, yield similar ages up to ~16.5 Ma, however some veins are as young as ca. 15.5 Ma and the grain-to-grain ages for a given sample can vary by up to ca. 0.5 Ma. Observed variations in age among the adularia crystals of a given rock sample indicate varying amounts of extraneous argon, and also loss of radiogenic <sup>40</sup>Ar, among the population of grains for a particular sample. The single-crystal results are interpreted to indicate a 16.5–15.5 Ma interval for formation of gold-bearing adularia veins in the region. The initiation and duration of this gold-forming event appears contemporaneous (within uncertainties) with the basaltic volcanism at the Steens Mountain section and an ensuing one-million-year episode of basaltic volcanism from multiple centers in the region (Brueseke et al., 2007).

Trace amounts of lead are alloyed with gold in the deposits studied. The isotopic compositions of this lead are not compatible with regional crustal units that host the gold ores, or the silicic igneous lithologies of the region, but have the same lead isotopic composition as basalts of the earliest Yellowstone plume (represented by the earliest lavas of the Columbia River basalt province, the Steens basalts, and Stonyford Volcanic Complex; Hanan et al., 2008). We propose that the gold studied and its traces of alloyed lead were derived together from the mantle, released from basaltic magma chambers of the province, and carried by low-density fluids into shallow geothermal systems during the earliest stages of Yellowstone hotspot magmatism.

© 2009 Elsevier B.V. All rights reserved.

## 1. Introduction

Layered mafic intrusions and large igneous provinces (LIPs) have well known associations with noble and base metal deposits, as in the Skaergaard-type intrusions and the Bushveld complex, and the extensive native copper ores formed in basalts of the Midcontinent Rift System of the Upper Peninsula of Michigan. Although gold deposits have not commonly been associated with LIPs, there is compelling evidence to indicate that gold is present in mantle plumes and can be transported to the crust within basaltic plume magmas. Native gold has been found in geologically young alkalic basaltic glass associated

with early flows of Kilauea, Hawaii (Sisson, 2003), providing unambiguous evidence for gold transport related to mantle plume magmatism. Native gold has also been reported as inclusions in olivine phenocrysts from picritic basalts of the Late Permian Emeishan LIP (Zhang et al., 2006). In a broader context for gold sourced in mantle-derived magmas, Kirk et al. (2003) present rhenium and osmium isotopic data to show that placer gold in the Witwatersrand basin (constituting about half of the known gold ores) appears to have a source in mantle lithologies or komatiites with an age of about 3.0 Ga, and to be associated with formation of the Kraaipan and Murchison greenstone belts. Thus, in widely differing stages of geologic time, there is evidence that gold can be derived from mantle magmatism, although the conditions and frequency of forming economic gold deposits from mantle sources is unclear.

Epithermal gold deposits of the Northern Great Basin (NGB) are spatially associated with the southeastern Oregon Plateau that was the

<sup>☆</sup> This paper arises from an abstract with the same title, by the authors above, that was presented in Theme Session #107 in a 2007 meeting of the Geological Society of America.

\* Corresponding author.

E-mail address: [hameswe@auburn.edu](mailto:hameswe@auburn.edu) (W. Hames).

locus for mid-Miocene initiation of Yellowstone hotspot magmatism as expressed by the Columbia River basalts (Fig. 1). Previous geochronologic studies have shown that the epithermal Au deposits of the region are also broadly mid-Miocene. The general coincidence in time and place of early Yellowstone magmatism and the high-grade 'bonanza' ores, among the richest gold deposits ever discovered, has prompted speculations and models linking these phenomena (e.g., Saunders et al., 1996; John, 2001). The basaltic magmatism has generally been considered to represent a source of heat to drive hydrothermal systems in the upper crust. The purpose of the present investigation is to refine estimates for the age of low-sulfidation epithermal 'bonanza' ores of this region to a level commensurate with recent high-precision age determinations for the CRB lavas (e.g., Brueseke et al., 2007), and interpret them in light of new lead isotopic data recently published by Kamenov et al. (2007). The latter indicates a mantle origin for the gold and a direct association with the early Yellowstone plume. We summarize this synthesis of  $^{40}\text{Ar}/^{39}\text{Ar}$  age and lead isotopic data with a new geodynamic model (from Saunders et al., 2008) for the bonanza ores of the region.

## 2. Previous work

Individual studies of the bonanza ore deposits of northwestern Nevada date back to the 1800's. Lindgren (1900) studied ores in the DeLamar-Silver City district of Idaho followed by detailed studies of Piper and Laney (1926) and Halsor et al. (1988). Lindgren (1898) also recognized the importance of hydrothermal potassium feldspar (first North

American documentation of adularia) to the epithermal ore-forming processes at DeLamar, and Lindgren (1915) further described the National Deposit in Humboldt County, Nevada. Studies by Vikre (1985, 1987, 2007) in the National district (and the Buckskin National deposit) were some of the first of Northern Great Basin epithermal ores to incorporate modern concepts about epithermal/geothermal systems. The discovery of the Sleeper deposit in the mid-1980's sparked new exploration interest for epithermal ores in the NGB (Saunders, 1990; Conrad et al., 1993; Saunders, 1994; Saunders and Schoenly, 1995; Nash et al., 1995). Recent studies of other epithermal precious metal deposits in the region, including Hog Ranch (Bussey, 1996), Midas (Leavitt et al., 2004), Mule Canyon (John et al., 2003), Ivanhoe (Wallace, 2003), and Seven Troughs (Hudson et al., 2006), and an overview of regional deposits by John (2001) provide a substantial body of data on NGB epithermal deposit geology, mineralogy, geochemistry, and geochronology. Unger (2008) completed a combined geochemical and  $^{40}\text{Ar}/^{39}\text{Ar}$  geochronologic investigation of epithermal ores in the Northern Great Basin and Silver City district of Idaho, and his work forms much of the basis for the present study.

### 2.1. Low-sulfidation epithermal precious metal systems

Many regional studies, as cited above, have established a number of general characteristics of low-sulfidation epithermal precious metal deposits in the NGB, including their relationship to extensional tectonism and bimodal volcanism. Epithermal systems form at shallow

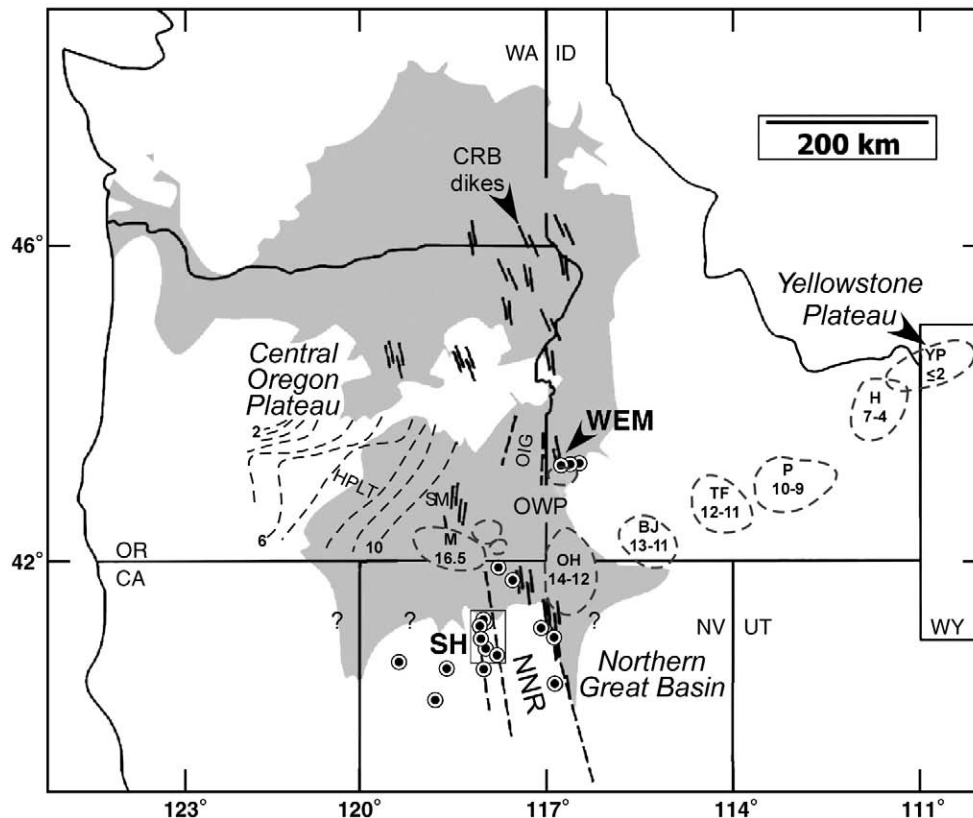


**Fig. 1.** Locations of epithermal gold deposits (bulleted circles) of the Northern Great Basin of Nevada and the Silver City district of Idaho in the context of the approximate extent of mid-Miocene flood basalts (the lightly shaded region, after Hart and Carlson, 1985; Camp and Ross, 2004) and select geologic features of the northwestern United States (map adapted from Pierce and Morgan, 1992, and Brueseke et al., 2007). Note that the southern extent of the mid-Miocene basalts is speculative. Silicic volcanic centers proposed to originate from Yellowstone hotspot migration are outlined by dashed lines: M – McDermitt caldera; OH – Owhyee-Humbolt volcanic field; TF – Twin Falls volcanic field; P – Picabo volcanic field; H – Heise volcanic field; YP – Yellowstone Plateau volcanic field. Ages for the silicic volcanic centers (generally rounded to the nearest million years and are intended to be inclusive) are based on compilations of Pierce and Morgan (1992), Morgan and McIntosh (2005), and Brueseke et al. (2007), with the addition of the ca. 16.5 Ma age for the McDermitt caldera from Henry et al. (2006). Long dashed lines represent major flood basalt dike swarms and eruptive loci. The westward-younging High Plains Lava Trend (HPLT) is also shown, with approximate isochrons shown as short-dashed lines with ages in Ma (from Jordan et al., 2004). Other abbreviations: OIG, Oregon–Idaho graben; NNR, Northern Nevada Rift; CRB, Columbia River basalt; WEM, War Eagle Mountain (part of the Owyhee mountains); OWP, Owyhee Plateau; SH, Slumbering Hills; SM, Steens Mountain. The inset indicates the map area for the Slumbering Hills in Fig. 3.

depths (<2 km) and low temperatures (<300 °C) and are classified as high-sulfidation, intermediate-sulfidation, and low-sulfidation based on ore mineralogy, alteration, and gangue mineral assemblages (Hedenquist and Lowenstern, 1994; John, 2001; Simmons et al., 2005). Low-sulfidation hydrothermal systems are generally associated with bimodal (basalt–rhyolite) or intermediate composition volcanism in a wide range of extensional tectonic settings (e.g., Sillitoe and Hedenquist, 2003). The ore-forming fluids in low-sulfidation hydrothermal systems have a low-salinity, have near-neutral pH, and are sulfide-dominated reducing (Hedenquist and Lowenstern, 1994). Low-sulfidation deposits most often form distal from the magmatic heat source (Sillitoe, 1989). These deposits are shallowly emplaced and easily eroded, thus few deposits older than Tertiary age are known.

The ore textures for low-sulfidation epithermal precious metal deposits have been well documented by a number of deposit-specific and overview studies as noted in the previous studies cited above. Colloform banded-veins, attributed to multiple pulses of mineralizing fluids, have been reported at many well known deposits. Alternating layers of quartz, chalcedony, adularia, calcite, clay, electrum, Ag-selenides, Ag-sulfides, Ag-sulfosalts, and/or base metal sulfides are typical. Adularia encrustations on open fractures are a common texture at the Jumbo, New Alma, Sandman and Ten Mile deposits in this study, and similar textures have been reported at Martha Hill, New Zealand (Simmons et al., 2005). Electrum dendrite textures are common, as is the deposition of Au and Ag minerals in 'sluice box textures' on the leeward side of quartz grains, indicating that Au and Ag were transported as colloids and deposited rapidly from supersaturated fluids (Saunders 1994; Saunders et al., 1996). Naumanite (Ag<sub>2</sub>Se), when present in these ores, also occurs with colloidal textures. Bladed calcite and its pseudomorphic replacement by quartz are also common, and are considered indicators of boiling in epithermal systems (Simmons and Christensen, 1994).

## 2.2. Precious metal source

The ultimate source of the precious metals in low-sulfidation epithermal systems is an issue that has been debated for over one hundred years. The two most common theories propose that metals either are leached from country rocks or derived from magmas. A previous study by John (2001), of mid-Miocene low-sulfidation epithermal deposits in the Northern Great Basin, determined these deposits are related to a mantle-derived anhydrous bimodal volcanic assemblage of mid-Miocene age. However, John (2001) indicates that the precise role that magmas had in the formation of these deposits "remains ambiguous" (p. 1846). A sedimentary origin for metals was inferred in some relatively recent deposit models (e.g. Nash et al., 1995; John et al., 2003).

It has also been suggested that basaltic rather than rhyolitic magmas may be responsible for Au-bearing fluids and there is some geochemical and isotopic data to support this theory (Noble et al., 1988; Connors et al., 1993; Kamenov et al., 2007). Native gold has been reported in very young basanite glass deposited on the submarine flank of Kilauea, Hawaii (Sisson, 2003). Native gold has also been discovered as an inclusion phase in olivine from picritic basalts of the Late Permian to Triassic Emeishan large igneous province of southwestern China (Zhang et al., 2006), which is associated with Late Permian rifting of the south China platform and considered broadly contemporaneous with the Siberian traps (Lo et al., 2002). These studies provide unambiguous evidence that gold can be transported to the crust from the mantle in mafic magmas derived from deep mantle hotspot plumes and erupted in rift-related flows of large igneous provinces.

The Hedenquist and Lowenstern (1994) model links epithermal precious metal deposits in subduction-related magmatic arcs to hydrothermal porphyry systems, and indicates magmatic fluids are important contributors to epithermal hydrothermal systems in such

settings. Later work has shown that magmatic fluids can transport Au from the porphyry environment into shallower epithermal systems (Heinrich et al., 2004; Heinrich, 2005). Deep hydrothermal waters at an actively-forming low-sulfidation Au deposit at Luise volcano at Lihir Island, Papua New Guinea contain extremely high levels of dissolved Au as bisulfide complexes (Simmons and Brown, 2006), which suggests that epithermal Au deposits could form in time spans of tens of thousands of years, or less (Heinrich, 2006).

## 2.3. Regional geology

The complex geologic history of the Northern Great Basin has resulted in numerous mineralizing events and deposit types. During the Nevadan, Elko, Sevier, and Laramide orogenies (Mesozoic to early Cenozoic), east-dipping subduction beneath western North America resulted in accretion of island arc terranes to the west in California and Cordillera-wide contraction from west to east, as well as widespread calc-alkaline magmatism throughout the Northern Great Basin (John, 2001). A transition to extension occurred in the late Eocene, possibly due to the removal of the subducted Farallon plate from the North American lithosphere (Cline et al., 2005). Concurrent initiation of high-K calc-alkaline magmatism and formation of most Carlin-type Au deposits occurred between 42 and 36 Ma (Cline et al., 2005). Although strong temporal and spatial relationships exist, the role of magmatism in the formation of Carlin-type deposits is still debated (see discussion in Muntean et al., 2001). Beginning about 17 Ma, extension became more widespread and along with coincident bimodal volcanism created the Basin and Range physiography of the region today (John, 2001).

The earliest stages of bimodal volcanism, including that associated with the northern Nevada rift (NNR), have been attributed to back-arc extension and/or the impingement of the Yellowstone hotspot with the upper crust (e.g., Brueseke et al., 2007). Early workers noted the association of basalt dike swarms with a single prominent magnetic anomaly, which represents the NNR (Zoback and Thompson, 1978; Zoback et al., 1994). Further work by Ponce and Glen (2002) identified three additional linear aeromagnetic highs, which they interpret to be subparallel rifts related to the NNR. All of these rifts are spatially associated with mid-Miocene bimodal volcanic centers. A strong spatial link between the rifts and mid-Miocene epithermal Au–Ag deposits exists (Ponce and Glen, 2002) and rift-related igneous activity is reported to have occurred predominately between 16.5 and 15 Ma (John et al., 2000). It has also been suggested that the development of the NNR and a number of other large-scale fractures in northern Nevada are related to the Yellowstone hotspot (Zoback and Thompson 1978; Zoback et al., 1994; Pierce et al., 2002; Glen and Ponce, 2002). Recent detailed studies of the Santa Rosa–Calico Range, the host of the National district, suggest that volcanism (at least in that study area) involves numerous intermediate compositions and is not strictly bimodal as previously thought (Brueseke and Hart, 2004). Basaltic volcanism in the Santa Rosa–Calico Range as well as eruption of the Steens Mountain basalt occurred from 16.73 ± 0.04 to 14.3 ± 0.38 Ma and from 16.58 ± 0.18 to 15.51 ± 0.28 Ma respectively (Brueseke et al., 2007). These ages are some of the earliest for mid-Miocene bimodal volcanism in the Great Basin and may reflect the initiation of the Yellowstone hotspot in the region.

## 2.4. Geochronology of low-sulfidation epithermal deposits

A mid-Miocene (17–13 Ma) time frame for bimodal volcanism and low-sulfidation epithermal Au–Ag deposits has been established by a number of studies using K/Ar and Ar/Ar methods in the Northern Great Basin to date various gangue minerals in ore veins and associated volcanic lithologies (see summaries in Conrad et al., 1993; John, 2001; Kamenov et al., 2007). However, the bulk-sample (K/Ar and <sup>40</sup>Ar/<sup>39</sup>Ar) techniques used in the previous studies yielded

relatively broad age constraints, hampered to a degree by difficulties in resolving the potential effects of extraneous argon or partial argon loss. The present study utilizes single-crystal analytical methods to better resolve the distribution of ages recorded by adularia within single samples.

### 2.5. The Yellowstone plume as a gold source: lead isotopic evidence

Lead is a common ore metal and can be alloyed with gold and silver. Thus, lead isotopes can provide information for the source of precious metal ores (Pettke and Frei, 1996; Kamenov et al., 2007). At first consideration, all lithologies in the region must be considered as potential sources for the precious metals in Northern Nevada, including local metasedimentary rocks, rhyolites, mafic lavas, and the lithospheric mantle. Miocene to recent volcanic activity in the region extends from the Oregon Plateau, through the Snake River Plain, to the Yellowstone Plateau (Fig. 1) and is represented by the Columbia River Basalt group, and bimodal volcanic deposits of the Snake River Plain and Yellowstone Plateau (for example, Pierce and Morgan, 1992; Camp, 1995; Pierce et al., 2002; Shervais and Hanan, 2008; Pierce and Morgan, 2009—this issue).

A number of studies have proposed that the onset of volcanic activity at ca. 16 Ma is related to the initial interactions of a mantle plume with the overriding lithosphere (e.g., Pierce and Morgan, 1992; Geist and Richards 1993; Hanan et al., 2008). The Miocene to recent basaltic lavas, including the basalts of the CRB have Pb isotopic signatures that are variable but generally consistent with a mantle plume origin, while data for Snake River Plain and Yellowstone volcanic centers indicate a mainly subcontinental lithosphere origin of the magmas (Hanan et al., 2008). Hanan et al. (2008) showed that ancient subcontinental lithosphere superimposes its isotopic signature on basaltic melts of the Snake River Plain and Yellowstone volcanic centers. As partial melts derived from the local Proterozoic to Archaean subcontinental mantle lithosphere are strongly enriched in Pb (compared to typical mantle plume melts) they would

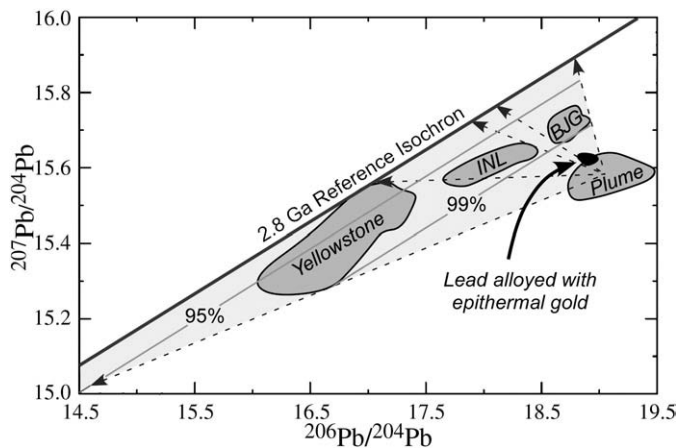


**Fig. 2.** Isotopic ratios of lead alloyed with epithermal gold from deposits in Northern Nevada (from Kamenov et al., 2007) compared with the lead isotopic compositions of time- and distance-transgressive basalts formed from the migrating Yellowstone hotspot, with a reference 2.8 Ga isochron representing the lead isotopic signature of the underlying regional lithosphere (the figure and lead isotopic data for basalts and lithosphere are simplified from data presented by Wooden and Mueller, 1988, and Hannan et al., 2008). Partial melts derived from plume-source mantle will shift toward an Archaean signature (as along vectors) with small degrees of lithospheric contamination (e.g., simulated shifts to 99% and 95% plume magma shown, corresponding to 1% to 5% assimilation of lithospheric partial melts). The isotopic composition of lead alloyed with epithermal gold is most similar to that inferred for the plume magmas. Distinct fields of lead isotopic composition for basalts with varying degrees of lithospheric contamination are indicated for the Yellowstone plateau, the eastern Snake River Plain (Idaho National Laboratory, INL), and the Bruneau, Jarbidge and Glens Ferry area eruptive centers (BJG).

dominate the isotopic signature of the plume lavas if present (see Hanan et al. 2008; Fig. 2). Basaltic lavas from Yellowstone, the eastern Snake River Plain (Idaho National Laboratory), the Bruneau-Jarbidge eruptive center, and the Glens Ferry area have Pb isotopic signatures that indicate lithospheric contamination and are distinct from the Yellowstone plume (Hanan et al., 2008). The original plume Pb isotopic signature (Fig. 2) is preserved in the earliest volcanism represented by the CRB, Steens basalts, and Stonyford Volcanic Complex (Hanan et al. 2008).

Kamenov et al. (2007) reported that the isotopic composition of traces of lead alloyed with native gold and electrum from several ores and deposits near the earliest eruptive centers of the Yellowstone plume are very similar to the isotopic composition inferred for the plume (Fig. 2). Some of the local mafic lavas sampled in the region of northwestern Nevada in our recent work (Kamenov et al., 2007) also yield lead isotopic compositions similar to those obtained for the gold and as defined for the earliest Yellowstone plume (e.g., Hanan et al., 2008; Fig. 2). The isotopic composition of lead alloyed in naumanite is similar to that of electrum, indicating that some metalloids (specifically selenium) are derived from the same source as the lead alloyed with gold (Kamenov et al., 2007). The lead isotopes in gold are distinct from lead in the regional metasedimentary rocks and rhyolites (which tend to be very radiogenic; see Kamenov et al., 2007), and also distinct from the progressively younger and more easterly basalts of the Yellowstone Plume (that record increasing degrees of contamination with lithospheric partial melts; Hanan et al., 2008). Even minor incorporation of lead from the local subcontinental lithospheric mantle would predictably have a strong effect on the Pb isotopic compositions of the lead alloyed with gold (Fig. 2). Thus, the regional lithosphere (including rhyolites, metamorphic rocks, lithospheric mantle and tholeiitic basalts of the Snake River Plain) cannot be implicated as providing source(s) of the lead found alloyed with epithermal gold. The similarity of the isotopic composition for lead alloyed with gold in epithermal deposits of northern Nevada to that inferred for the plume is interpreted to indicate that the early Yellowstone mantle plume was the most likely source for the precious metals in the deposits. Hofstra and Creaser (2009) tested this hypothesis, and they found that ratios of Re–Os isotopes in gold from the Sleeper deposit (see location in Fig. 3A relative to samples of this study) are similar to Re–Os isotopes of the earliest Columbia River basalts and thus to the inferred plume. The collective isotopic dataset is, therefore, compatible with a genetic origin for the epithermal gold in the deep mantle.

An alternative hypothesis can be offered, for the purpose of discussion, to allow that the primitive lead and Re–Os isotopes are indeed from a mantle plume source, but requiring that the gold is from a crustal source and was alloyed with the lead and other isotopes during vein formation. However, as Hannan et al. postulated for the basalts of the Snake River Plain, we infer that addition of any small amount of lithospheric lead would be expected to significantly shift the compositions we observe in the gold away from the plume signature. Thus, we reject this hypothesis because it would require the addition of gold from a crustal source that was completely devoid of any trace of lead.

### 3. Single-crystal laser $^{40}\text{Ar}/^{39}\text{Ar}$ geochronology

All  $^{40}\text{Ar}/^{39}\text{Ar}$  dating of the present study was performed in the Auburn Noble Isotope Mass Analysis Laboratory (ANIMAL). Adularia ( $\text{KAlSi}_3\text{O}_8$ ) was chosen as the mineral to be dated based on the fact that it is rich in K, and a common gangue mineral that is often intimately associated with the Au/Ag minerals. Piper and Laney (1926) described the association of adularia with ores in the vicinity of Silver City, Idaho as follows: “Valencianite [adularia] is abundant in apparently all the veins on Florida Mountain, regardless of the type of rock in which they occur. Beautiful examples were found in the veins in basalt. It occurs as well developed crystals, occasionally nearly an

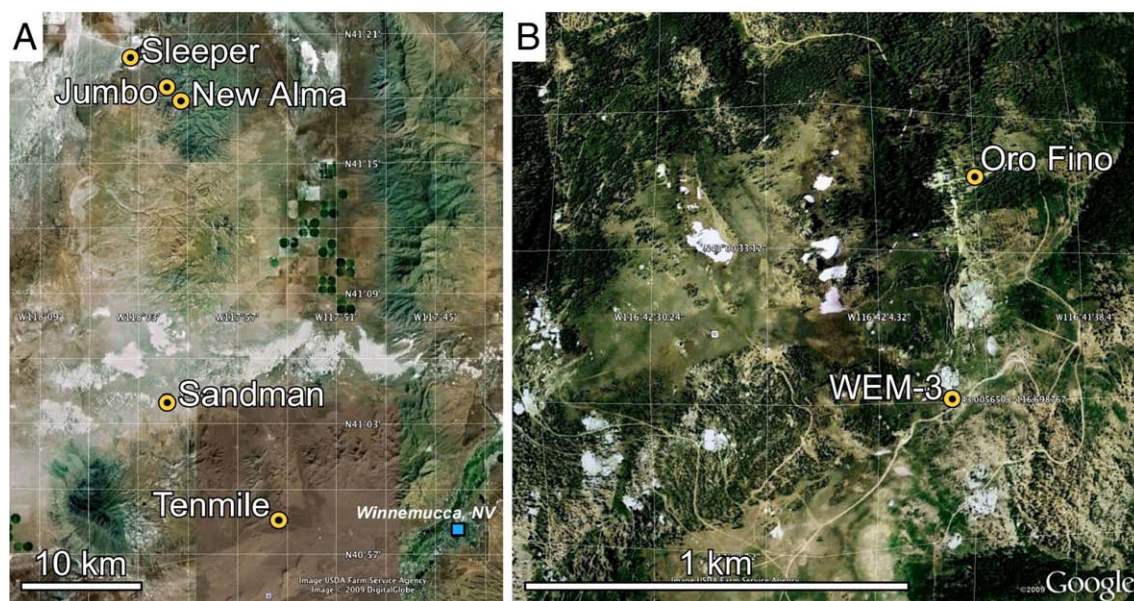


**Fig. 3.** A) A map of Slumbering Hills area gold deposits (modified from Wendt, 2003; see Fig. 1 for the inset map location of the Slumbering Hills). B) Topographic map of sample locations for OF-1 and WEMS3-1 taken from historic workings on War Eagle Mountain (see Fig. 1 for the regional location of War Eagle Mountain). Contour lines are labeled in feet. Field coordinates for samples of this study are provided in the Appendix (Created in Google Earth).

inch in diameter, as a coating on walls and on fragments of various kinds in the brecciated veins, and often contains inclusions of chalcopyrite, naumanite, argentite, and other ore minerals or is coated by them." Adularia with intergrown Au/Ag minerals was obtained from four sites in and around the Slumbering Hills, NV (Jumbo, New Alma, Sandman, and Ten Mile) as well as two sites on War Eagle Mountain, ID (Fig. 3). Field relationships observed in the present study between adularia and basalt in the Oro Fino vein of the Silver City district are presented in Fig. 4, and representative samples of adularia analyzed in this study are shown in Fig. 5.

Each sample was crushed and sieved to a 14–20 mesh size fraction for hand picking. Individual crystals or cleavage fragments were selected to be generally free from visible inclusions of other phases. Crystals with visible alteration (e.g., cloudy, turbid crystals in contrast to those that were clear) were avoided in sample selection to the maximum extent

possible, and, when present, visible alteration effects are discussed with results for each sample. All samples were washed in dilute HF prior to analysis to remove any oxide or fine silicate (typically clay) coatings. Neutron irradiation for the production of  $^{39}\text{Ar}$  followed standard procedures as described by Dalrymple et al. (1981), using the central core facility of the McMaster Nuclear Reactor in Hamilton, Ontario. Crystals were placed in aluminum disks with the monitor FC-2 (age = 28.02 Ma, Renne et al., 1998) along with reagent grade  $\text{K}_2\text{SO}_4$  and  $\text{CaF}_2$  as flux monitors. Following irradiation,  $^{40}\text{Ar}/^{39}\text{Ar}$  dating in ANIMAL was based on laser incremental heating of single adularia grains. For each sample, five single crystals were incrementally heated separately with an incremental heating schedule of 10–20 steps. Data reduction and assessment of statistical ages were accomplished through use of a custom Microsoft Excel application and Isoplot (Ludwig, 2003). Results were evaluated through use of standard isochron and age

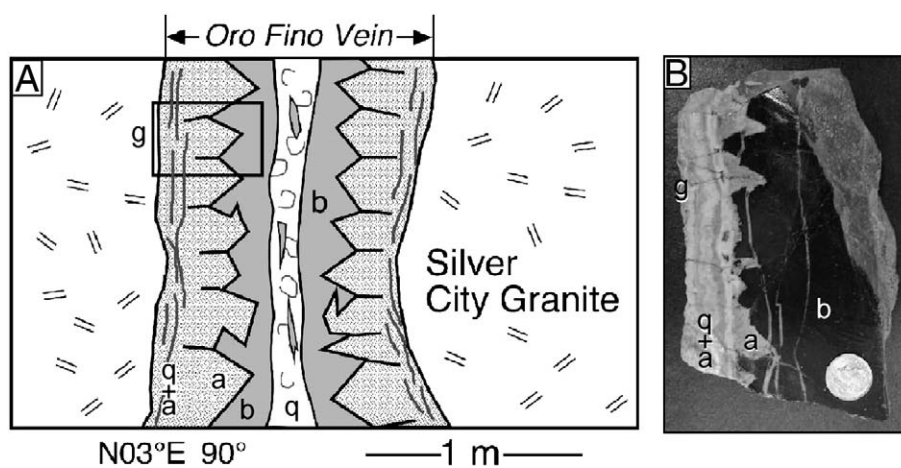


**Fig. 4.** A) A sketch of a portion of the Oro Fino vein in cross section oriented perpendicular to strike (vein attitude indicated) with the relative relationships of the Silver City granite (g) and zoning within the vein that includes quartz (q), adularia (a), basalt (b), and a central zone dominated by hydrothermal quartz (q). The vein is ~1 m wide where sampled (as indicated) but the size of adularia crystals in the sketch is exaggerated and not to scale. B) Photograph of a slab cut from a piece of the vein (dime for scale) in the orientation and location schematically represented by the box in A. Note that the left side of the slab contains a thin portion of granite, followed by a zone of quartz and adularia, then coarse subhedral adularia, followed by basalt (near the vein center).

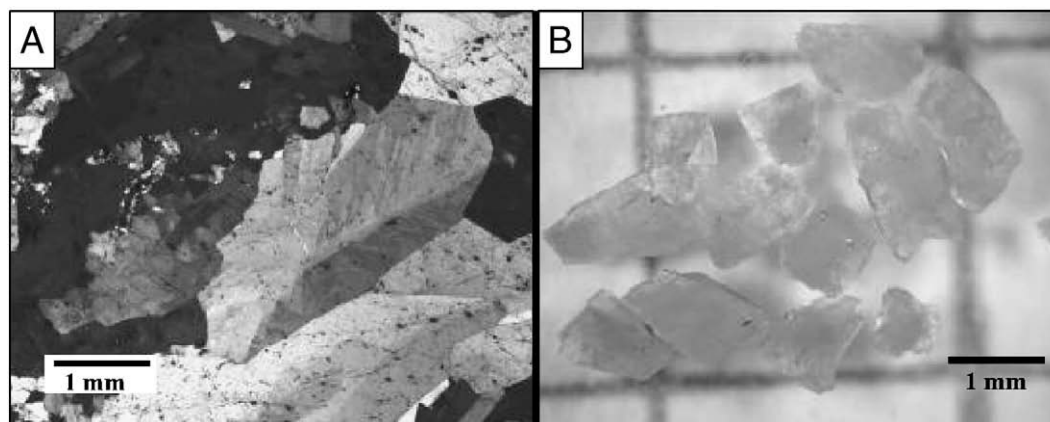


**Fig. 5.** A) Photomicrograph of coarse adularia from the Jumbo mine (cross polarized illumination). B) Single crystals of adularia from the Jumbo mine, selected for  $^{40}\text{Ar}/^{39}\text{Ar}$  analysis by crushing and hand picking. Inclusions in these crystals contain visible gold. Crystals tend to break along grain boundaries and cleavage planes, and were examined in plane and cross-polarized illumination to select grains for analysis dominated by single crystals.

spectrum approaches for calculating single crystal ages. Generally, the analyses were highly radiogenic, with little correlated  $^{36}\text{Ar}$ , and thus the age spectra are preferred and presented in this study. Plateau were defined such that: the plateau increments constituted greater than 60% of the total  $^{39}\text{Ar}_K$  released in three or more contiguous heating steps, there is no resolvable slope among steps of the plateau, there are no outliers at the beginning or the end of the plateau, and the probability of fit for the steps is greater than 5%. All ages discussed in the text and presented in figures are at the 95% confidence level (although incremental heating steps are graphed with  $1\sigma$  errors). Full data tables and other notes regarding laboratory procedures are available in the [Appendix](#).

### 3.1. Results from the slumbering hills deposits

#### 3.1.1. Jumbo

The Jumbo deposit sits in the northern Slumbering Hills near the Sleeper mine and a deposit referred to as New Alma ([Fig. 3A](#)). A study by [Conrad et al. \(1993\)](#), using K/Ar methods, determined that adularia in veins from Jumbo had an age of 17.3 Ma. However, the bulk-sample total-fusion techniques used in that study were not capable of resolving extraneous, non-atmospheric ('excess') argon, which could produce an older age. Our new laser  $^{40}\text{Ar}/^{39}\text{Ar}$  data for this sample were first summarized in [Kamenov et al. \(2007\)](#). In the present study, five adularia crystals were analyzed and three of these yield plateau ages ([Fig. 6A](#)). Plateau ages for these three crystals overlap within uncertainties and yield a combined age of  $16.54 \pm 0.04$  Ma (at the 95% confidence level, MSWD = 0.23). We interpret this age to represent the crystallization of adularia in the Jumbo vein as sampled. The other two crystals have variable amounts of extraneous argon, as evidenced by initial release of relatively large amounts of  $^{40}\text{Ar}$ , and a resolvable increase in age among successive heating increments ([Fig. 6A](#), and data of the [Appendix](#)). We infer that these results reflect the presence of extraneous  $^{40}\text{Ar}$  trapped in surface defects or in fluid inclusions, and that such extraneous argon is heterogeneously distributed among crystals of the sample.

#### 3.1.2. New Alma

The New Alma deposit occurs south of the Jumbo mine workings in the Slumbering Hills. All crystals were from one sample of a very thin (<3 cm thick) vein, and had a light coating of Fe- and Mn-oxides

developed during hydrothermal alteration or weathering. (These weathering products are volumetrically insignificant and very typical of minerals in the deposits studied, and were removed by washing in dilute HF acid prior to analysis.) Four of the five adularia crystals analyzed produced plateau ages that range from  $16.07 \pm 0.04$  to  $15.86 \pm 0.08$  Ma ([Fig. 6B](#)). The one crystal that did not produce a plateau age still yields individual heating increment ages that are consistent with the other samples. The variation in plateau ages among the crystals analyzed is greater than expected to arise solely from analytical precision.

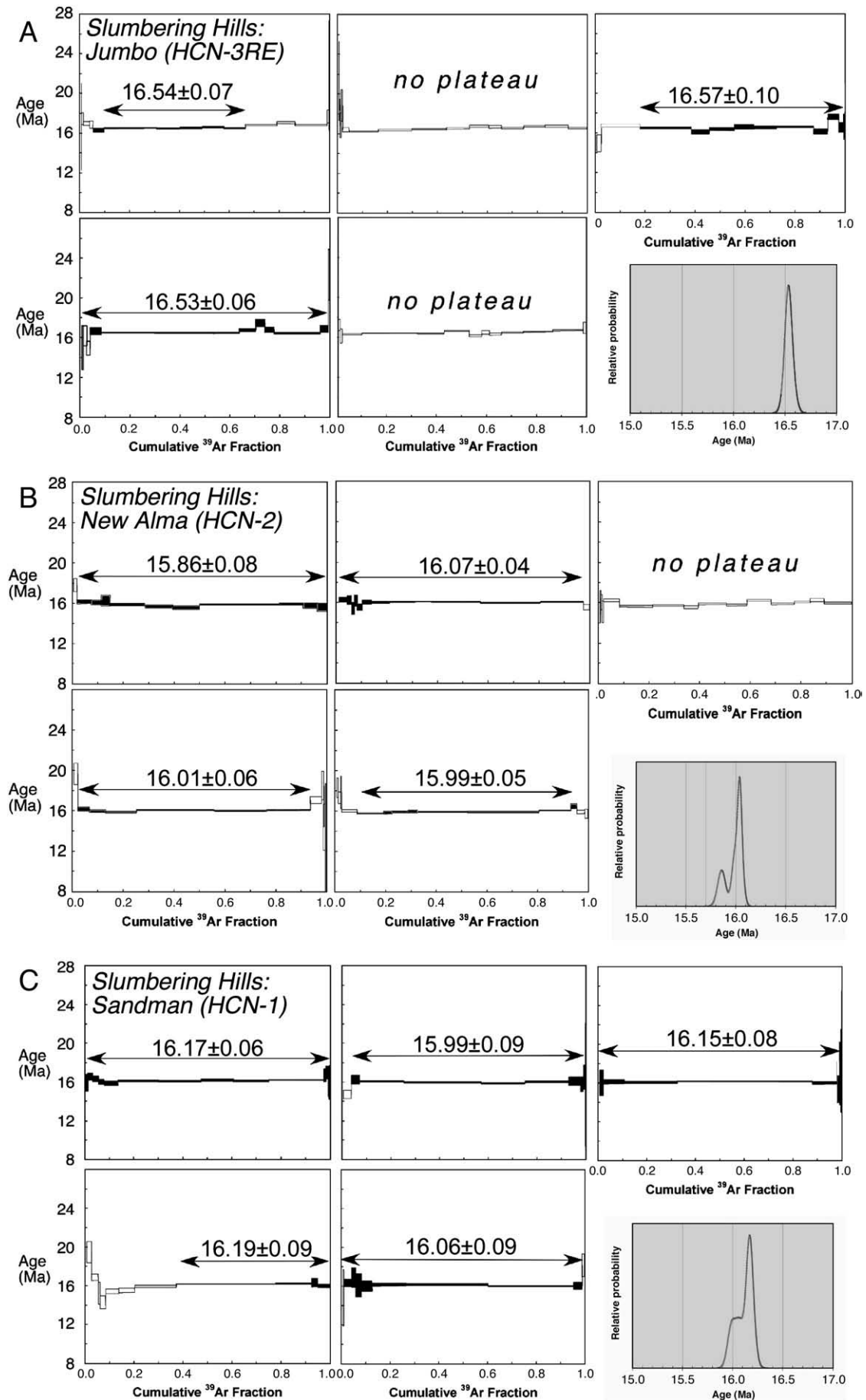
The vein sampled at New Alma is typical of all our samples from the Slumbering Hills, in that it is thin (less than a few centimeters wide), it does not show field or petrographic evidence for repeated opening and vein filling, or dissolution and re-precipitation, and its host lithologies were likely at a temperature below a few hundred degrees centigrade at the time of vein intrusion. Therefore, it is unlikely that a significant amount of time (such as 90–330 thousand years, considering the precision of measurement for these co-irradiated crystals) elapsed between the deposition of different crystals within the vein. We suggest that a degree of post-crystallization loss for radiogenic  $^{40}\text{Ar}$ , likely during late-stage circulation of hydrothermal fluids or surficial weathering, results in the spread of ages determined for New Alma, and that the maximum plateau age result of  $16.07 \pm 0.04$  Ma should be viewed as a minimum estimate for adularia crystallization in the deposit.

#### 3.1.3. Sandman

The Sandman deposit is in the southern pediment of the Slumbering Hills. The area has been the subject of a number of exploration projects and is currently being explored for epithermal precious metal mineralization. Some of the coarsest visible gold (up to 2 mm) observed in this study is present in adularia encrustations on fracture surfaces in silicified tuffaceous host rock.

Five crystals from sample HCN-1 were analyzed by incremental heating and produced plateau ages ([Fig. 6C](#)) with a range of  $16.19 \pm 0.09$  to  $15.99 \pm 0.09$  Ma. The weighted average age of the three oldest crystals is  $16.17 \pm 0.04$  Ma (MSWD = 0.19), and we suggest that this age should be considered as a minimum estimate of adularia crystallization in the deposit. (At the 95% confidence level, there is an ~82% chance that the variance of the three plateau ages is consistent with a normal distribution of errors in precision.) Adularia crystals from the Sandman

**Fig. 6.**  $^{40}\text{Ar}/^{39}\text{Ar}$  laser incremental heating release spectra for single crystals of adularia, with five crystals analyzed per sample, along with a probability plot for plateau ages of the sample. All crystals were of the 14–20 mesh size (1.2–0.75 mm). Increments defining plateau are shaded, and defined with standard criteria provided in [Isoplot \(Ludwig, 2003\)](#) and as discussed in the text. Data are plotted with  $1\sigma$  errors and plateau ages are presented and discussed in the text at the 95% confidence level. Full analytical data are presented in the [Appendix](#). A) Incremental heating data for crystals from the Jumbo deposit; B) data from the New Alma deposit; C) data from the Sandman deposit; D) data from the Ten Mile Deposit; E) data from War Eagle Mountain, and the Oro Fino vein; F) and data from War Eagle Mountain, for a vein in an unnamed adit referred to as 'Site 3'.



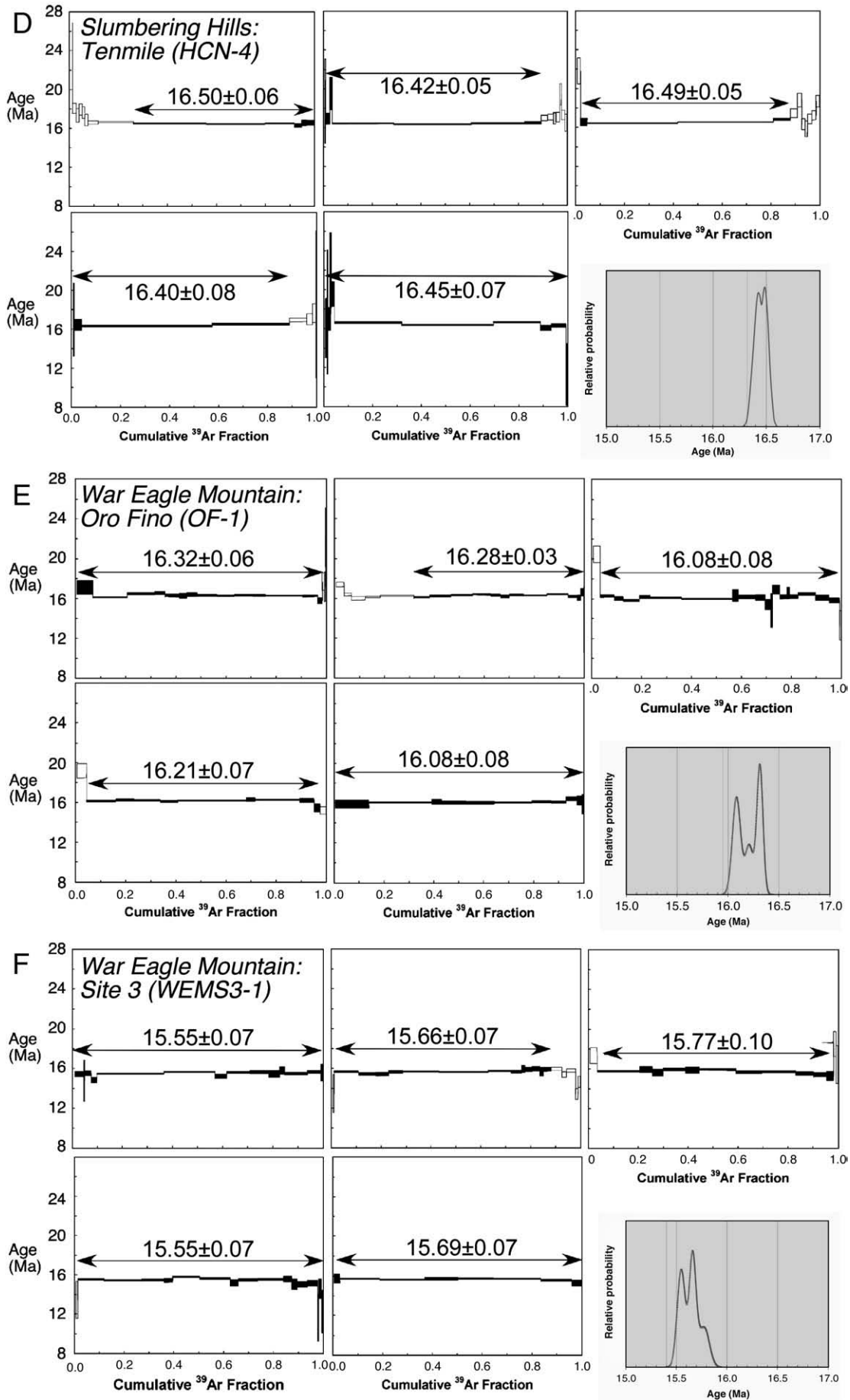


Fig. 6 (continued).

deposit typically have a thin coating of white clay, which also may reflect post-crystallization circulation of hydrothermal fluids. As was the case with the New Alma adularia, we interpret the two significantly younger ages from the Sandman adularia to reflect alteration that resulted in the loss of accumulated radiogenic  $^{40}\text{Ar}$ .

### 3.1.4. Ten Mile

The Ten Mile deposit is southeast of the Slumbering Hills and just to the north of Winnemucca, NV (Fig. 3A). The vein samples collected at the Ten Mile deposit are highly oxidized material with obvious coatings of Fe- and Mn-oxides. Plateau ages for five crystals (Fig. 6D) range from  $16.50 \pm 0.06$  to  $16.40 \pm 0.08$  Ma. The weighted average for all five crystals is  $16.46 \pm 0.05$  Ma (MSWD = 2.3, with a 6% probability of fit), a result statistically identical to that obtained for the Jumbo mine, that we interpret to reflect the minimum age for vein formation in the Ten Mile deposit.

### 3.1.5. War Eagle Mountain

War Eagle Mountain is in the Silver City district of southwestern Idaho. The area has been the site of precious metal mining for well over a hundred years, and scores of historic workings cover War Eagle Mountain (e.g., Fig. 3B). Previous work by Halsor et al. (1988), using K–Ar methods, determined that adularia from veins on War Eagle Mountain ranges in age from ~16.6 to 15.2 Ma. Samples for the present study were collected from a vein outcrop directly beneath the Oro Fino adit (WEM: Oro Fino), and another unnamed adit located ~0.5 km southwest (sample WEMS-3).

All of the samples were very fresh, and all ten of the crystals analyzed from these two samples yielded plateau ages. The sample from the Oro Fino vein yielded plateau ages ranging from  $16.32 \pm 0.06$  to  $16.08 \pm 0.08$  Ma (Fig. 6E). The weighted average of the oldest three plateau ages is  $16.28 \pm 0.08$  Ma (MSWD = 3.0, with a 5% probability of fit). We infer that the oldest ages for this sample are representative of a minimum age of vein formation, and that the slightly younger ages reflect argon loss from less retentive or altered crystals. Plateau ages from the unnamed adit (WEMS-3, Fig. 6F) are considerably younger than any other samples analyzed, and range from  $15.77 \pm 0.10$  to  $15.55 \pm 0.07$  Ma. The scatter of these age results is greater than expected analytically, indicating some degree of effects from extraneous argon or loss of radiogenic argon. Although the incremental heating analysis that yielded the oldest result (15.77 Ma) revealed extraneous, non-atmospheric argon in the initial and final heating steps (constituting about 5% of the total  $^{39}\text{Ar}$  released), such ‘excess’ argon is not evident in the other sample results. The probability distributions for ages determined for the Oro Fino sample and the sample from the unnamed adit (Figs. 6D and E) are distinct, a result that could indicate that there were multiple episodes of (gold-bearing) veins that formed within a relatively small region, or that the adularia from some samples (as WEMS-3) is susceptible to greater amounts of post-crystallization loss of radiogenic argon.

Ages determined in the present study are summarized in Fig. 7, along with recent age determinations for CRB lavas in the Steens Mountain section and from volcanic centers in the region (Brueseke et al., 2007). All of the plateau ages for adularia of the present study were used to construct the probability plot of the epithermal veins, with the result that the initial peak of their formation is at ~16.5 Ma, with continuing formation indicated until ca. 15.5 Ma. Most of these deposits formed in the approximate interval of 16.5–16.0 Ma (only the sample WEMS-3 yielded ages consistently younger than 16.0 Ma). The age range indicated by the probability distribution of the CRB lavas is very similar (Fig. 7). Thus, available geochronologic data are consistent with the same regional relationships of intensity of activity and timing for the formation of the bonanza-type Au deposits and the multiple eruptive events for the earliest basalts of the Yellowstone plume.

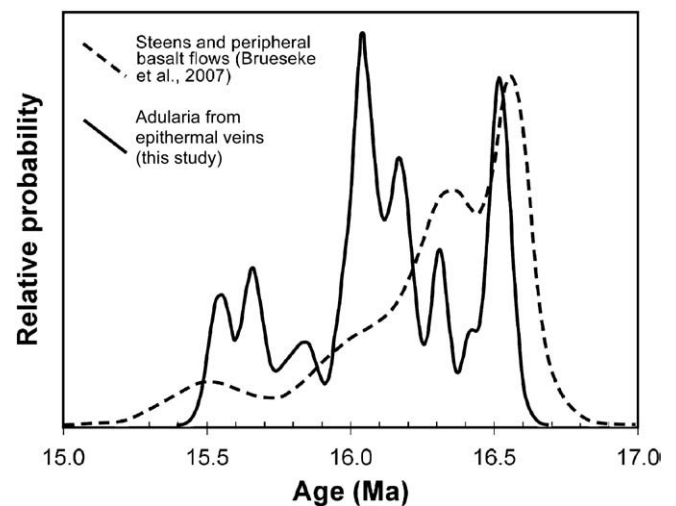
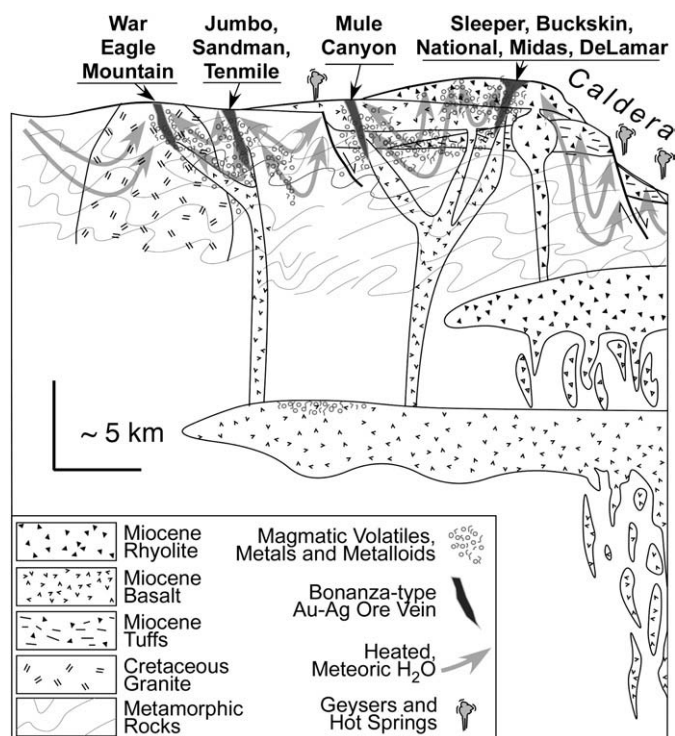


Fig. 7. Summary probability plot of all plateau ages for adularia determined in the present study (solid curve), and of ages determined for basalts of the southwestern Oregon plateau (dashed curve) including basalt flows in the Steens Mountain section (represented by the peak age of ca. 16.57 Ma as reported by Brueseke et al. (2007)).

## 4. A model for the genesis of Northern Great Basin epithermal deposits

Saunders et al. (1996) proposed a genetic link between the Yellowstone hotspot and the middle Miocene epithermal deposits of the NGB. John (2001) classified these ores as “extension-related” epithermal ores in the NGB to distinguish them from a separate class he termed “subduction-related” ores of western Nevada. However, John (2001) proposed the deposits were related to the middle Miocene bimodal volcanism and through-going structures such as the NNR. Although recognizing their relationship to bimodal volcanics in space and time, John (2001) proposed that there was no apparent direct connection to the magmas. The model proposed by John (2001) and John et al. (2003) for the genesis of these deposits was similar to that proposed by Nash et al. (1995). In that model, magma chambers principally served as a heat source to drive geothermal systems that leach metals, sulfur, and major elements from the wall rocks. The Pb isotopic data of the present study do not support the concept that gold or silver of the ores investigated were leached from the surrounding country rocks. A new genetic model for evolution of the ores (Saunders et al., 2008; Fig. 8) is based on: 1) present-day geology at Yellowstone National Park area; 2) Pb-isotope data of the present study; 3) our geologic observations about host rock controls on styles of mineralization for the group of middle Miocene epithermal ores; and 4) new and previous geochronology of ores and host rocks. This model (Fig. 8) depicts magma chambers of basalt overlain by rhyolite which fed the bimodal volcanism associated with the initial emergence of the YHS at about 16.5 Ma. We further propose that heat from these magmas (perhaps predominantly the rhyolitic magmas as at Yellowstone today) caused the formation of shallow geothermal systems that vented to the surface as hot springs and geysers. Acid volatiles provided by the magmas caused leaching of major elements (silica, Al, K, Na, Ca, etc.) from country rock to form hydrothermal veins and hot spring deposits at the surface. Locally, these barren geothermal systems evolved into precious metal ore depositing systems when low-density fluids were episodically released from the basaltic magma chambers into the shallow geothermal system. Recent research has shown that significant quantities of gold and sulfur can be transported in these low-density (e.g., “vapors”) fluids (Heinrich, 2005; Williams-Jones and Heinrich, 2005) that apparently can be absorbed by the shallow geothermal systems. We propose that this process was important in NGB epithermal ore formation, and that it essentially locks in the mafic magmatic Pb-isotope signature of the precious metal minerals in the epithermal ores (e.g., Kamenov et al., 2007). We interpret the multicyclic banding of electrum and silica (as in the bonanza ores of the Sleeper mine) to record the episodic release of



**Fig. 8.** Model for the genesis of the Northern Great Basin epithermal gold deposits (adapted from Saunders et al., 2008; deep crustal structure is based on the schematic cross section of the Yellowstone Caldera described by Lowenstern and Hurwitz (2008)). The model depicts a cross section for half of a caldera system, and indicates the host lithologies for various mines and deposits of the region. The topography and vertical scale of shallow geologic features (<5 km depth) in this schematic drawing are greatly exaggerated to show the context for various deposits discussed in the text.

gold to the shallow geothermal system. Because our model invokes a deep magmatic source of precious metals, the shallow country rocks are irrelevant to the metal budget, yet their composition does affect the styles of mineralization, vein and alteration mineralogy (Fig. 8). Finally, if the ores of the Silver City district in Idaho (Fig. 1) are considered with those in northwestern Nevada, their proposed association with the NNR (e.g., John, 2001) appears less strong. Thus, the structural control of the NNR might be a second order feature useful in localizing or exposing some ores, but the first order control on their origin is interpreted to correspond with the footprint of the underlying Yellowstone hotspot.

## 5. Conclusions

A number of lines of evidence suggest that mid-Miocene low-sulfidation epithermal precious metal mineralization in the Northern Great Basin is related to the initial development of the Yellowstone hotspot. The similarities in mineralogy and geochemistry among the Northern Great Basin deposits examined in this study indicate a common source of the major metal and metalloid ore components. The earliest volcanism associated with the CRB lavas of the Yellowstone hotspot occurs in the southwestern Oregon Plateau, that began at  $16.59 \pm 0.10$  Ma to  $16.55 \pm 0.1$  Ma and continued until ca. 15.5 Ma (Brueseke et al., 2007). The new  $^{40}\text{Ar}/^{39}\text{Ar}$  age for the Jumbo deposit of  $16.54 \pm 0.04$  Ma, and similar results for the Ten Mile deposit, indicate that the main and waning stages of epithermal gold mineralization in the region began during or shortly after the first CRB volcanism related to the Yellowstone hotspot.  $^{40}\text{Ar}/^{39}\text{Ar}$  ages of other samples in this study are interpreted to indicate that gold mineralization continued over a span of time comparable to the waning of CRB magmatism in the region.

The single-crystal  $^{40}\text{Ar}/^{39}\text{Ar}$  dating strategy of this study shows that effects of extraneous  $^{40}\text{Ar}$ , or  $^{40}\text{Ar}$  loss, are heterogeneously distributed

among the adularia crystals in these samples. Earlier published results for  $^{40}\text{Ar}/^{39}\text{Ar}$  incremental heating of 'bulk samples' (i.e. comprising several to tens of crystals) may lead to an average age for a population of crystals that is biased by heterogeneous effects of extraneous argon or loss of radiogenic argon. Thus, we infer that a single-crystal approach as utilized in this study is advantageous for determining the  $^{40}\text{Ar}/^{39}\text{Ar}$  age of coarse adularia.

The isotopic compositions of minute traces of lead alloyed with gold from the bonanza deposits in this region are generally incompatible with other crustal sources, but are very comparable to the mid-Miocene plume-related magmas of the Yellowstone hotspot province. We conclude that the gold of the epithermal ores of the Northern Great Basin originated in the mantle and was transported with plume magmas in the early Yellowstone hotspot.

## Acknowledgements

This work was partially supported by grants from the Mineral Resources Program of the U.S. Geological Survey and the National Science Foundation (EAR 0838208) to J. Saunders and W. Hames. G. Kamenov was supported through the course of this work through a grant from the National Science Foundation. The authors wish to thank M. Brueseke for encouragement and helpful suggestions in the project, and W. Utterback for assistance in sample collecting. Comments from two anonymous reviewers greatly improved the manuscript. The authors also wish to express appreciation for the thorough reviews and expert comments provided by the journal editors.

## Appendix A. Supplementary data

Supplementary data associated with this article can be found, in the online version, at doi: [10.1016/j.jvolgeores.2009.07.020](https://doi.org/10.1016/j.jvolgeores.2009.07.020).

## References

- Brueseke, M.E., Hart, W.K., 2004. The physical and petrologic evolution of a multi-vent volcanic field associated with Yellowstone-Newberry volcanism. *Eos, Transactions of AGU* 87, V53A-605.
- Brueseke, M.E., Heizler, M.T., Hart, W.K., Mertzman, S.A., 2007. Distribution and geochronology of Oregon Plateau (U.S.A.) flood basalt volcanism: the Steens Basalt revisited. *Journal of Volcanology and Geothermal Research* 161, 187–214.
- Bussey, S.D., 1996. Gold mineralization and associated rhyolitic volcanism at the Hog Ranch District, northwest Nevada. *Proceedings of the International Symposium on the Geology and Ore Deposits of the America Cordillera*, pp. 181–210. Reno, NV.
- Camp, V.E., 1995. Mid-Miocene propagation of the Yellowstone mantle plume head beneath the Columbia River basalt source region. *Geology* 23, 435–438.
- Camp, V.E., Ross, M.E., 2004. Mantle dynamics and genesis of mafic magmatism in the intermontane Pacific Northwest. *Journal of Geophysical Research* 109, B08204.
- Cline, J.S., Hofstra, A.H., Muntean, J.L., Tosdal, R.M., Hikey, K.A., 2005. Carlin-type gold deposits in Nevada: critical geologic characteristics and viable models. *Economic Geology 100th Anniversary* 451–484 Volume.
- Connors, K.A., Noble, D.C., Bussey, S.D., Weiss, S.I., 1993. Initial gold contents of silicic volcanic rocks: bearing on the behavior of gold in magmatic systems. *Geology* 21, 937–940.
- Conrad, J.E., McKee, E.H., Rytuba, J.J., Nash, J.T., Utterback, W.C., 1993. Geochronology of the Sleeper deposit, Humboldt County, Nevada: epithermal gold-silver mineralization following silicic flow-dome complex. *Economic Geology* 88, 317–327.
- Dalrymple, G.B., Alexander, E.C., Lanphere, M.A., and Kraker, G.P., 1981. Irradiation of samples for  $^{40}\text{Ar}/^{39}\text{Ar}$  dating using the geological survey TRIGA reactor. USGS Professional Paper 1176, 55 pp.
- Geist, D., Richards, M., 1993. Origin of the Columbia River plateau and Snake River plain: deflection of the Yellowstone plume. *Geology* 21, 789–792.
- Glen, J.M.G., Ponce, D.A., 2002. Large-scale fractures related to inception of the Yellowstone hotspot. *Geology* 30, 647–650.
- Halsor, S.P., Bornhorst, T.J., Beebe, M., Richardson, K., Strowd, W., 1988. Geology of the DeLamar silver mine, Idaho—a volcanic dome complex and associated hydrothermal system. *Economic Geology* 83, 1159–1169.
- Hanan, B.B., Shervais, J.W., Vetter, S.K., 2008. Yellowstone plume-continental lithosphere interaction beneath Snake River Plain. *Geology* 36, 51–54.
- Hart, W.K., Carlson, R.W., 1985. Distribution and geochronology of Steens Mountain-type basalts from the northwestern Great Basin. *Isotopes* 43, 5–10.
- Hedenquist, J.W., Lowenstern, J.B., 1994. The role of magmas in the formation of hydrothermal ore deposits. *Nature* 370, 519–527.
- Heinrich, C.A., 2005. The physical and chemical evolution of low-salinity magmatic fluids at the porphyry to epithermal transition; a thermodynamic study. *Mineralium Deposita* 39, 864–889.

- Heinrich, C.A., 2006. How fast does gold trickle out of volcanoes? *Science* 314, 263–264.
- Heinrich, C.A., Driesener, T., Stefansson, A., Seward, T.M., 2004. Magmatic vapor contraction and the transport of gold from the porphyry environment to epithermal ore deposits. *Geology* 32, 761–764.
- Henry, C.D., Castor, S.B., McIntosh, W.C., Heizler, M.T., Cuney, M., Chemillac, R., 2006. Timing of oldest Steens basalt magmatism from precise dating of silicic volcanic rocks, McDermitt Caldera and Northwest Nevada volcanic field. *Eos Trans. AGU* 87, 52.
- Hofstra, A.H., Creaser, R.A., 2009. Re–Os isotope results for electrum from three low sulfidation epithermal Au–Ag deposits in the Great Basin. *Geological Society of America Abstracts with Programs* 41 (6), 20.
- Hudson, D.M., John, D.A., Fleck, R.J., 2006. Geology, geochemistry, and geochronology of epithermal deposits in the Seven Troughs district, Pershing County, Nevada. *Geological Society of Nevada, Special Publication* 42, 110–126.
- John, D.A., 2001. Miocene and early Pliocene epithermal gold silver deposits in the northern Great Basin, western USA: characteristics, distribution, and relationship to magmatism. *Economic Geology* 96, 1827–1853.
- John, D.A., Wallace, A.R., Ponce, D.A., Fleck, R., and Conrad, J.E., 2000. New perspectives on the geology and origins of the northern Nevada rift. *Geological Society of Nevada, Geology and Ore Deposits 2000, the Great Basin and Beyond Symposium*, May 15–18, 2000, Reno–Sparks, Nevada, Proceedings, pp. 127–154.
- John, D.A., Hofstra, A.H., Fleck, R.J., Brummer, J.E., Saderholm, E.C., 2003. Geologic setting and genesis of the Mule Canyon low-sulfidation epithermal gold–silver deposit, north-central Nevada. *Economic Geology* 98, 425–464.
- Jordan, B.T., Grunder, A.L., Duncan, R.A., Deino, A.L., 2004. Geochronology of age-progressive volcanism of the Oregon High Lava Plains: implications for the plume interpretation of Yellowstone. *Journal of Geophysical Research* 109, B10202. doi:10.1029/2003JB002776.
- Kamenov, G.D., Saunders, J.A., Hames, W.E., Unger, D., 2007. Mafic magmas as sources for gold in middle-Miocene epithermal deposits of Northern Great Basin, USA: evidence from Pb isotopic compositions of native gold. *Economic Geology* 102, 1191–1195.
- Kirk, J., Ruiz, J., Chesley, J., Tittle, S., 2003. The origin of gold in South Africa. *American Scientist* 91, 534–541.
- Leavitt, E.D., Spell, T.L., Goldstrand, P.M., Arehart, G.G., 2004. Geochronology of the Midas low-sulfidation gold–silver deposit, Elko County Nevada. *Economic Geology* 99, 1665–1686.
- Lindgren, W., 1898. Hydrothermal potassium feldspar in gold ores from De Lamar, Idaho. *American Journal of Science (Fourth Series)* 30, 418–420.
- Lindgren, W., 1900. The gold and silver veins of the Silver City, De Lamar, and other mining districts in Idaho: US Geological Survey 20th Annual Report, Part 3, pp. 65–256.
- Lindgren, W., 1915. Geology and mineral deposits of the National District, Nevada. U.S. Geological Survey Bulletin 601.
- Lo, C.H., Chung, S.L., Lee, T.Y., Wu, G.Y., 2002. Age of the Emeishan flood magmatism and relations to Permian–Triassic boundary events. *Earth and Planetary Science Letters* 198, 449–458.
- Lowenstern, J.B., Hurwitz, S., 2008. Monitoring a supervolcano in repose: heat and volatile flux at the Yellowstone Caldera. *Elements* 4, 35–40.
- Ludwig, K.R., 2003. User's manual for Isoplot, v. 3.0, a geochronological tool kit for Microsoft Excel. Berkeley Geochronological Center, Berkeley, CA, Special Publication no. 4.
- Morgan, L.A., McIntosh, W.C., 2005. <sup>40</sup>Ar/<sup>39</sup>Ar ages of silicic volcanic rocks in the Heise volcanic field, eastern Snake River Plain, Idaho: timing of volcanism and tectonism. *Geological Society of America Bulletin* 117 (3/4), 288–306.
- Muntean, J., Tarnocai, C., Coward, M., Rouby, D., Jackson, A., 2001. Styles and restorations of Tertiary extension in north-central Nevada. *Geological Society of Nevada Special Publication* 33, 55–69.
- Nash, J.T., Utterback, W.C., Trudel, W.S., 1995. Geology and geochemistry of Tertiary volcanic host rocks, Sleeper gold–silver deposit, Humboldt County, Nevada. U.S. Geological Survey Bulletin 2090.
- Noble, D.C., McCormack, J.K., McKee, E.H., Silberman, M.L., Wallace, A.B., 1988. Time of mineralization in the evolution of the McDermitt caldera complex, Nevada–Oregon, and relation to middle-Miocene mineralization in the Great Basin to coeval regional basaltic activity. *Economic Geology* 83, 859–863.
- Pettke, T., Frei, R., 1996. Isotope systematics in vein gold from Brusson, Val d'Ayas (NW Italy). Pb/Pb evidence for a Piemonte metaophiolite Au source. *Chemical Geology* 27, 111–124.
- Pierce, K.L., Morgan, L.A., 1992. The track of the Yellowstone hotspot: volcanism, faulting, and uplift. In: Link, P.K., Kuntz, M.A., Platt, L.W. (Eds.), *Regional geology of Eastern Idaho and Western Wyoming: Geological Society of America Memoir*, vol. 179, pp. 1–53.
- Pierce, K.L. and Morgan, L.A., 2009. Is the track of the Yellowstone hotspot driven by a deep mantle plume?—Review of volcanism, faulting, and uplift in light of new data. *Journal of Volcanology and Geothermal Research*, this issue.
- Pierce, K.L., Morgan, L.A., and Saltus, R., 2002. Yellowstone plume head: postulated relations to the Vancouver slab, continental boundaries, and climate. In: Bill Bonnichsen, C.M. White, and Michael McCurry (Editors), *Tectonic and Magmatic Evolution of the Snake River Plain Volcanic Province*. Idaho Geological Bulletin 30, p. 5–33.
- Piper, A.M., Laney, F.B., 1926. Geology and metalliferous resources of the region about Silver City, Idaho. Idaho Bureau of Mines and Geology Bulletin 11, 165.
- Ponce, D.A., Glen, J.M.G., 2002. Relationship of epithermal gold deposits to large-scale fractures in northern Nevada. *Economic Geology* 97, 3–9.
- Renne, P.R., Swisher, C.C., Deino, A.L., Karner, D.B., Owens, T.L., DePaolo, D.J., 1998. Intercalibration of standards, absolute ages, and uncertainties in <sup>40</sup>Ar/<sup>39</sup>Ar dating. *Chemical Geology* 145, 117–152.
- Saunders, J.A., 1990. Colloidal transport of gold and silica in epithermal precious metal systems: evidence from the Sleeper deposit, Humboldt County, Nevada. *Geology* 18, 757–760.
- Saunders, J.A., 1994. Silica and gold textures at the Sleeper deposit, Humboldt County, Nevada: evidence for colloids and implications for ore-forming processes. *Economic Geology* 89, 628–638.
- Saunders, J.A., Schoenly, P.A., 1995. Boiling, colloid nucleation and aggregation, and the genesis of bonanza gold mineralization at the Sleeper Deposit, Nevada. *Mineralium Deposita* 30, 199–211.
- Saunders, J.A., Schoenly, P.A., Cook, R.B., 1996. Electrum disequilibrium crystallization textures in volcanic-hosted bonanza epithermal gold deposits: Proceedings of the International Symposium on the Geology and Ore Deposits of the America Cordillera: (Reno, NV) p. 173–179.
- Saunders, J.A., Unger, D.L., Kamenov, G.D., Hames, W.E., Utterback, W.C., 2008. Genesis of mid-Miocene Yellowstone-hotspot-related bonanza epithermal Au–Ag deposits, Northern Great Basin region, USA. *Mineralium Deposita* 43, 715–734.
- Shervais, J.W., and Hanan, B.B., 2008. Lithospheric topography, tilted plumes, and the track of the Snake River–Yellowstone hot spot: *Tectonics*, v. 27, TC5004. doi:10.1029/2007/TC002181, 17 p.
- Sillitoe, R.H., 1989. Gold deposits in western Pacific island arcs; the magmatic connection. *Economic Geology Monographs* 6, 274–291.
- Sillitoe, R.H., Hedenquist, J.W., 2003. Linkages between volcanotectonic settings, ore-fluid compositions, and epithermal precious metal deposits. *Society of Economic Geologists Special Publication* 10, 315–343.
- Simmons, S.F., Brown, K.L., 2006. Gold in magmatic hydrothermal solutions and the rapid formation of a giant ore deposit. *Science* 314, 288–291.
- Simmons, S.F., Christensen, B.W., 1994. Origins of calcite in a boiling geothermal system. *American Journal of Science* 294, 361–400.
- Simmons, S.F., White, N.C., and John, D.A., 2005. Geological characteristics of epithermal precious and base metal deposits: *Economic Geology 100th Anniversary Volume*, p. 485–522.
- Sisson, T.W., 2003. Native gold in a Hawaiian alkalic magma. *Economic Geology* 98, 643–648.
- Unger, D.L., 2008. Geochronology and geochemistry of mid-Miocene bonanza low-sulfidation epithermal ores of the northern Great Basin, U.S.A. Unpublished MS thesis, Auburn University, 134 p.
- Vikre, P.G., 1985. Precious metal vein system in the National district, Humboldt County, Nevada. *Economic Geology* 80, 360–393.
- Vikre, P.G., 1987. Paleohydrology of Buckskin Mountain, National district, Humboldt County, Nevada. *Economic Geology* 82, 934–950.
- Vikre, P.G., 2007. Sinter-vein correlations at Buckskin Mountain, National District, Humboldt County, Nevada. *Economic Geology* 102, 193–224.
- Wallace, A.R., 2003. Geology of the Ivanhoe Hg–Au district, Northern Nevada: influence of Miocene volcanism, lakes, active faulting on epithermal mineralization. *Economic Geology* 98, 409–424.
- Wendt, C.J., 2003. Nevada mineral trends. Nevada Bureau of Mines and Geology, Open-File Report OF03-2 (a 1:1,000,000-scale map).
- Williams-Jones, A.E., Heinrich, C.A., 2005. Vapor transport of metals and the formation of magmatic-hydrothermal ore deposits. *Economic Geology* 100, 1287–1312.
- Wooden, J.L., Mueller, P.A., 1988. Pb, Sr, Nd isotopic compositions of a suite of Late Archean, igneous rocks, eastern Beartooth Mountains: implications for crust–mantle evolution. *Earth and Planetary Science Letters* 87, 59–72.
- Zhang, Z., Mao, J., Wang, F., Piranjo, F., 2006. Native gold and native copper grains enclosed by olivine phenocrysts in a picrite lava of the Emeishan large igneous province, SW China. *American Mineralogist* 91, 1178–1183.
- Zoback, M.L., Thompson, G.A., 1978. Basin and Range rifting in northern Nevada: clues from a mid-Miocene rift and its subsequent offsets. *Geology* 6, 111–116.
- Zoback, M.L., McKee, E.H., Blakely, R.J., Thompson, G.A., 1994. The northern Nevada rift: regional tectono-magmatic relations and middle Miocene stress direction. *Geological Society of America Bulletin* 106, 371–382.